J Mater Sci: Mater Med (2009) 20:1869–1879
DOI 10.1007/s10856-009-3755-8

Nucleation and growth of calcium phosphates in the presence of fibrinogen on titanium implants with four potentially bioactive surface preparations. An in vitro study

Anna Arvidsson · Fredrik Currie · Per Kjellin · Young-Taeg Sul · Victoria Stenport

Received: 16 November 2008 / Accepted: 15 April 2009 / Published online: 5 May 2009

Abstract The aim of this study was to compare the nucleating and crystal growth behaviour of calcium phosphates on four types of potentially bioactive surfaces, using the simulated body fluid (SBF) model with added fibrinogen. Blasted titanium discs were modified by alkali and heat treatment, anodic oxidation, fluoride treatment, or hydroxyapatite coating. The discs were immersed in SBF with fibrinogen for periods of 3 days and 1, 2, 3 and 4 weeks. The topography, morphology, and chemistry of the surfaces were evaluated with optical interferometry, scanning electron microscopy/energy dispersive X-ray analysis (SEM/EDX), and x-ray photoelectron spectroscopy (XPS), respectively. All surface modifications showed early calcium phosphate formation after 3 days, and were almost completely covered by calcium phosphates after 2 weeks. After 4 weeks, the Ca/P ratio was approximately 2.0 for all surface groups except the fluoride modified surface, which had a Ca/P ratio of 1.0–1.5. XPS measurements of the nitrogen concentration, which can be interpreted as an indirect measure of the protein content, reached a peak value after 3 days immersion and decreased thereafter. In conclusion, the results in the present study, when compared to earlier SBF studies without proteins, showed that fibrinogen stimulates calcium phosphates formation. Furthermore, no pronounced differences could be detected between blasted controls and the potentially bioactive specimens.

A. Arvidsson (✉) · F. Currie · P. Kjellin · Y.-T. Sul · V. Stenport
Institute of Surgical Sciences, Göteborg University, Gothenburg, Sweden
e-mail: anna.arvidsson@biomaterials.gu.se

1 Introduction

One way of enhancing bone formation around dental implants is to perform surface topographical modifications [1, 2]. The surface roughness of implants has been suggested to be important for vascularisation and ingrowth of bone [3], as well as for biomechanical interaction [4, 5]. As discussed by Hansson [6], a biomechanical coupling between implant and bone can be achieved by a rough surface provided that sufficient bone–implant interfacial shear strength is obtained. Since the metallic implant is significantly stronger than the bone tissue, wide "bone plugs" between narrow implant structures give greater bone–implant interfacial shear strength than narrow bone plugs between wide implant structures [6]. Furthermore, nanostructures have been shown to stimulate osteoblast adhesion [7, 8].

However, it is also possible that bone anchorage could be obtained by means of biochemical bonding, a characteristic possibly related to bioactive implants [5]. Bioactivity has been defined as "the characteristic of an implant material which allows it to form a bond with living tissues" [9]. Theoretically, the advantage of bioactive implants is that biochemical attachment is rapid; that is, it acts at a time when proper biomechanical interlocking has not yet been developed, and consequently the implants may become fixed more rapidly [5]. Accelerated and enhanced bone formation might be of particular value in cases where implants will come under immediate load, or in clinically compromised situations.

Titanium surface modifications which create potentially bioactive surfaces include alkali and heat treatment [10, 11], anodic oxidation with electrolytes containing phosphorous, sulphur, calcium, or magnesium ions [12], sodium plasma immersion ion implantation and deposition

[13], calcium phosphate coatings or particle deposition [14, 15], and fluoride treatment [16–18]. Bioactivity has so far been impossible to prove [5], but different indications for bioactivity have been presented. For example, when fluoride treated or anodically oxidised implants are removed from rabbit bone, the rupture generally occurs in the bone tissue rather than at the bone–implant interface [12, 16]. Other researchers have evaluated bioactivity by examining nucleation and growth of apatite after immersion of implants in simulated body fluid (SBF) [19].

SBFs are buffers with ion concentrations approximately equal to those of human blood plasma [19, 20]. The first phase of bone healing around a newly installed bone-anchored implant occurs in the blood [21], and thus the SBF model is also of interest in the context of dental implants. Furthermore, a review by Kokubo and Takadama [22] concluded that there is a correlation between apatite formation in SBF and in vivo bone bioactivity: "a material able to have apatite form on its surface in SBF can bond to living bone through the apatite layer formed on its surface in the living body, as long as the material does not contain any substance that induces toxic or antibody reactions". The SBF model is frequently used in current research, and is described in an international standard (ISO 23317:2007E, "Implant for surgery: in vitro evaluation for apatite-forming ability of implant materials"). In a previous study performed by our research group, differences between controls and potentially bioactive surface types appeared at SBF immersion times of 1 and 2 weeks [23]. There were also differences between blasted titanium and potentially bioactive surfaces when albumin was added to the SBF [24]. However, the influence of other plasma proteins on nucleation and growth of calcium phosphates has not been extensively investigated.

During wound healing, blood platelets aggregate and form a plug that is reinforced by fibrin threads formed from fibrinogen as a result of the coagulation process [25]. The blood clot not only plugs injured blood vessels, but functions as a matrix for the inflammatory and connective tissue cells. Although the role of fibrinogen in the coagulation system is well-known, its effect in the mineralisation process has been less studied. Different complexes and molecules such as collagen, non-collagenous proteins, phospholipids, and proteolipids have been hypothesised to possess nucleating ability [26]. The hypothesis of the present study is that proteins have a clear impact on the mineralisation process and that the nucleation and growth of calcium phosphates will be altered when fibrinogen, which is a naturally occurring plasma protein, is added to the SBF. Thus, the aim of this study was to compare the nucleation and growth of calcium phosphates on four different and potentially bioactive surface modifications, immersed in SBF with fibrinogen.

2 Materials and methods

2.1 Surface preparations

A total of 90 circular discs (Ø: 8 mm, thickness: 3 mm) of commercially pure titanium (grade 3) were included in the present study. In order to increase the surface roughness, the specimens were blasted with Al_2O_3 powder with a particle size of 75 μm. Thereafter, the specimens were ultrasonically cleaned in diluted Extran MA01 and absolute ethanol, respectively, and dried at 60°C for 24 h. The specimens were then divided into five groups, one of which ($n = 18$) served as a control and was not subjected to any surface treatment prior to the SBF immersion. The other groups of specimens were treated with the following surface preparations.

2.1.1 Alkali and heat treatment

Alkali and heat treatment was performed as described in the literature [27–29]. The specimens ($n = 18$) were soaked in 5 M aqueous NaOH for 24 h at 60°C and then gently washed with distilled water before being left to dry for 24 h at 40°C. The specimens were then heated to 600°C by increasing the temperature by 5°C/min in air in an electrical furnace (Bitatherm, Bita Laboratory Furnaces, Israel), and were kept at 600°C for 1 h before being allowed to cool to room temperature in the furnace.

2.1.2 Anodic oxidation

The samples ($n = 18$) were prepared in a mixed electrolyte containing magnesium ions, such as magnesium sulphate, using the micro-arc oxidation method in galvanostatic mode [30]. The electrochemical cell was composed of two platinum plates as cathode with a titanium anode at the centre. Currents and voltages were continuously recorded at intervals of 1-s by an IBM computer interfaced with a DC power supply. The content of ripple was controlled to less than 0.1%. The surface properties of the oxidised group were characterised as a magnesium titanate consisting of 9 at.% Mg, 3.4 μm of oxide thickness, 24% porosity of porous structure, and anatase plus rutile of crystal structure [31].

2.1.3 Fluoride treatment

Samples ($n = 18$) were fluoride treated as per the technique of Ellingsen [16]: they were immersed in an aqueous solution of 0.95 M NaF, washed twice in distilled water for 30 s, and then allowed to dry spontaneously at room temperature. X-ray photoelectron spectroscopy (XPS) was used to confirm the presence of fluorine.

2.1.4 Hydroxyapatite coating

A hydroxyapatite coating was obtained by dipping the titanium discs ($n = 18$) into a stable solution containing surfactants, water, organic solvent, and crystalline nanoparticles of hydroxyapatite with a Ca/P ratio of 1.67. The diameter of the hydroxyapatite particles was approximately 10 nm. After the dipping procedure the discs were dried for half an hour in open air, allowing the organic solvent to evaporate. This was followed by a heat treatment at 550°C for 5 min under nitrogen atmosphere in order to remove all dispersing agents. The nitrogen atmosphere was used in order to protect the titanium surface from further oxidation. The treatment resulted in a very thin hydroxyapatite coating on the titanium surface (less than 100 nm thick), as measured with XPS and scanning electron microscopy (SEM).

2.2 SBF + fibrinogen immersion

The revised SBF (r-SBF) described by Oyane et al. [20] was used. It was prepared by dissolving 5.403 g NaCl, 0.740 g $NaHCO_3$, 2.046 g Na_2CO_3, 0.225 g KCl, 0.230 g $K_2HPO_4 \cdot 3H_2O$, 0.311 g $MgCl_2 \cdot 6H_2O$, 11.928 g 2-(4-(2-hydroxyethyl)-1-piperazinyl)ethanesulfonic acid (HEPES), 0.293 g $CaCl_2$, and 0.072 g Na_2SO_4 in 1000 ml distilled water. HEPES was dissolved in 100 ml distilled water before being added to the solution. Fibrinogen was thereafter added to a concentration of 0.1 g/l, and the final pH was adjusted to 7.4 at 37°C with 1.0 M NaOH. All chemicals were obtained from VWR International (Stockholm, Sweden), with the exception of fibrinogen (Fibrinogen Type I–S from bovine plasma), which was obtained from Sigma Aldrich (Schnelldorf, Germany).

Each specimen was immersed in 25 ml r-SBF + fibrinogen in separate sealed polystyrene vials and kept at 37°C. Once every week the r-SBF + fibrinogen were changed to freshly prepared buffer. After immersion for 3 days ($n = 3$), 1 week ($n = 3$), 2 weeks ($n = 3$), 3 weeks ($n = 3$), and 4 weeks ($n = 3$), the SBF + fibrinogen immersion was interrupted and the specimens were thoroughly rinsed with distilled water to remove any loosely attached calcium phosphate material. The specimens were thereafter dried at room temperature and sealed in dry vials while awaiting surface analysis. Three samples of each type of surface were not immersed in any SBF + fibrinogen, thus serving as controls within each surface preparation group.

2.3 Evaluation of surfaces

2.3.1 Optical interferometry

Specimens were topographically analysed after SBF + fibrinogen immersion with an optical interferometer (MicroXam^{TM}, PhaseShift, Tucson, USA). Due to poor optical reflectivity of specimens immersed in SBF for longer periods, only control specimens and specimens immersed in SBF for 3 and 7 days were analysed in this way. With a 50× objective and a zoom factor of 0.625, the measurement area was 260 × 200 μm^2. Three areas were measured on each specimen. The vertical and lateral resolutions of this equipment with the current settings were 0.1 nm and 0.5 μm, respectively. Before calculation of the topographical parameters, errors of form and waviness were excluded using a Gaussian high pass filter with a size of 50 × 50 μm^2. The surface roughness was characterised with the following topographical parameters [32]:

S_a = Arithmetic mean height deviation from a mean plane [μm].
S_{ds} = Density of summits, i.e., the number of summits of a unit sampling area [mm^{-2}].
S_{sk} = Skewness, i.e., a measure of symmetry of the surface height distribution with respect to a mean/reference plane.
S_{dr} = Developed interfacial area ratio, i.e., the ratio of the increment of the interfacial area of a surface over the sampling area [%].
S_{ci} = Core fluid retention index, i.e., the ratio of the void volume of the unit sampling area at the core zone (5–80% bearing area) over the root-mean-square deviation. A high value indicates a good fluid retention in the core zone, and values typically range from 0 to slightly more than 2.

2.3.2 Scanning electron microscopy/energy dispersive X-ray analysis (SEM/EDX)

A LEO Ultra 55 FEG SEM equipped with an Oxford Inca EDX system, operating at 7 kV, was used for the SEM analyses. The samples were examined without surface sputtering. Micrographs were recorded at different magnifications to investigate both the surface coverage degree and the morphologies of the crystals. The atomic composition was monitored using EDX analysis on two levels of magnification. Analyses at a low magnification were performed on a major part of the sample to describe a mean value of the atomic composition. The EDX instrument was calibrated with a standard hydroxyapatite sample in order to ensure that the correct calcium and phosphorous ratios were measured.

EDX results were compared to results from an earlier study [23] with the same surface modification groups and model settings; with the only difference that fibrinogen was not added to the buffer. The comparison was based on multivariate statistical analysis by utilising General MANOVA (Minitab®, Minitab Inc., USA).

2.3.3 X-ray photoelectron spectroscopy (XPS)

A more surface sensitive chemical analysis was obtained by XPS (PHI 5000 ESCA System, Perkin–Elmer Wellesley, USA) with an operating angle of 45° at 300 W using a MgK excitation source. An average was calculated from two separate analyses at the approximate middle and close to the edge of two specimens.

3 Results

3.1 Optical interferometry

The topographical results are presented in Table 1. As seen from the mean S_a values, all surface groups were classified as moderately rough [5]. For most surface groups, the density of summits (S_{ds}) increased after 3 days immersion.

Table 1 Topographical parameters calculated from optical interferometer analyses

SBF immersion time (days)	Surface type	Topographical parameters				
		S_a (μm)	S_{ds} ($\times 10^3$ mm^{-2})	S_{dr} (%)	S_{ci}	S_{sk}
0 days	B	1.04 (0.04)	143 (4)	47 (2)	1.37 (0.03)	−0.53 (0.14)
	AH	1.03 (0.04)	210 (6)	55 (3)	1.40 (0.05)	−0.31 (0.20)
	AO	1.02 (0.05)	173 (4)	55 (2)	1.37 (0.03)	−0.52 (0.15)
	F	1.00 (0.04)	148 (5)	43 (3)	1.41 (0.03)	−0.34 (0.17)
	HA	1.05 (0.04)	130 (3)	51 (3)	1.37 (0.03)	−1.21 (0.29)
3 days	B	1.02 (0.05)	209 (15)	66 (12)	1.34 (0.09)	−2.63 (1.83)
	AH	1.05 (0.04)	214 (7)	72 (2)	1.41 (0.03)	−0.32 (0.11)
	AO	0.96 (0.09)	223 (10)	65 (10)	1.41 (0.06)	−0.49 (0.26)
	F	1.00 (0.09)	215 (17)	60 (9)	1.44 (0.03)	−0.28 (0.08)
	HA	1.00 (0.05)	217 (10)	62 (5)	1.41 (0.04)	−1.02 (0.65)
7 days	B	1.06 (0.05)	182 (37)	60 (6)	1.35 (0.05)	−1.94 (1.08)
	AH	1.03 (0.06)	221 (4)	68 (9)	1.43 (0.03)	−0.45 (0.41)
	AO	1.00 (0.09)	185 (9)	55 (3)	1.36 (0.05)	−0.58 (0.14)
	F	0.96 (0.06)	231 (23)	70 (13)	1.44 (0.07)	−0.32 (0.26)
	HA	1.02 (0.06)	160 (37)	49 (6)	1.40 (0.04)	−0.57 (0.17)

B blasted titanium, *AH* alkali and heat treated, *AO* anodically oxidised, *F* fluoride treated, *HA* hydroxyapatite coated. The figures represent means ($n = 9$); standard deviations are given within parentheses

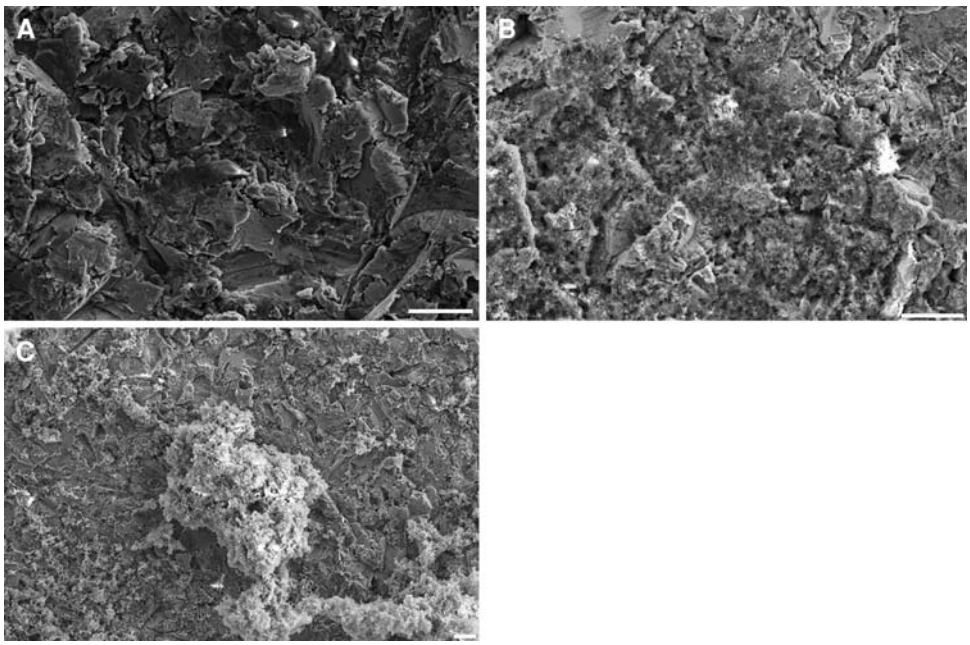

Fig. 1 SEM images of blasted specimens, before (**a**) and after SBF + fibrinogen immersion for 3 days (**b**) and 2 weeks (**c**). *Bars* correspond to 10 μm

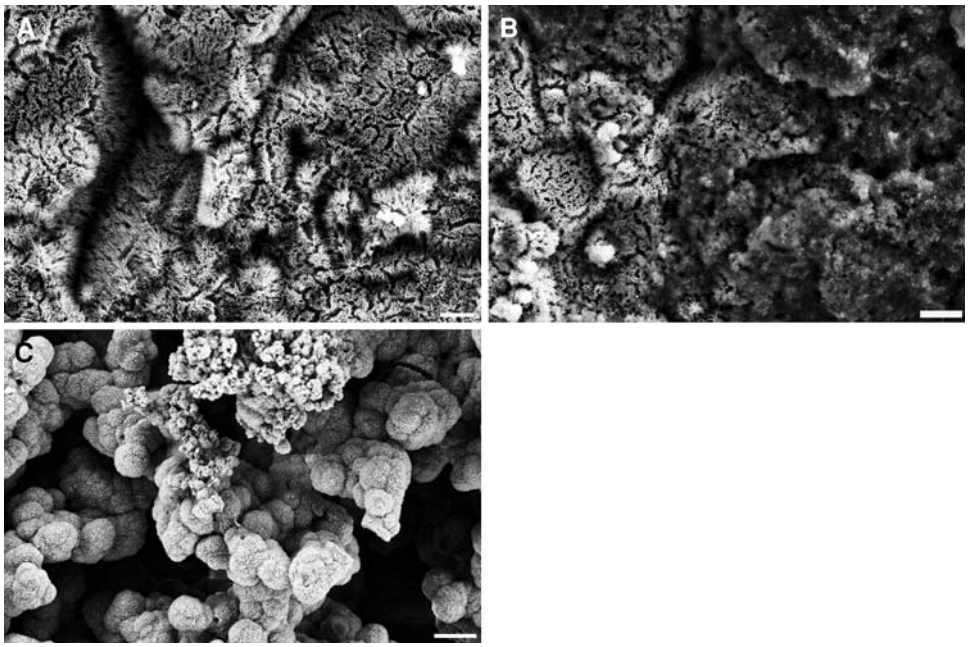

Fig. 2 SEM images of alkali and heat treated specimens, before (**a**) and after SBF + fibrinogen immersion for 3 days (**b**) and 2 weeks (**c**). *Bars* correspond to 3 μm

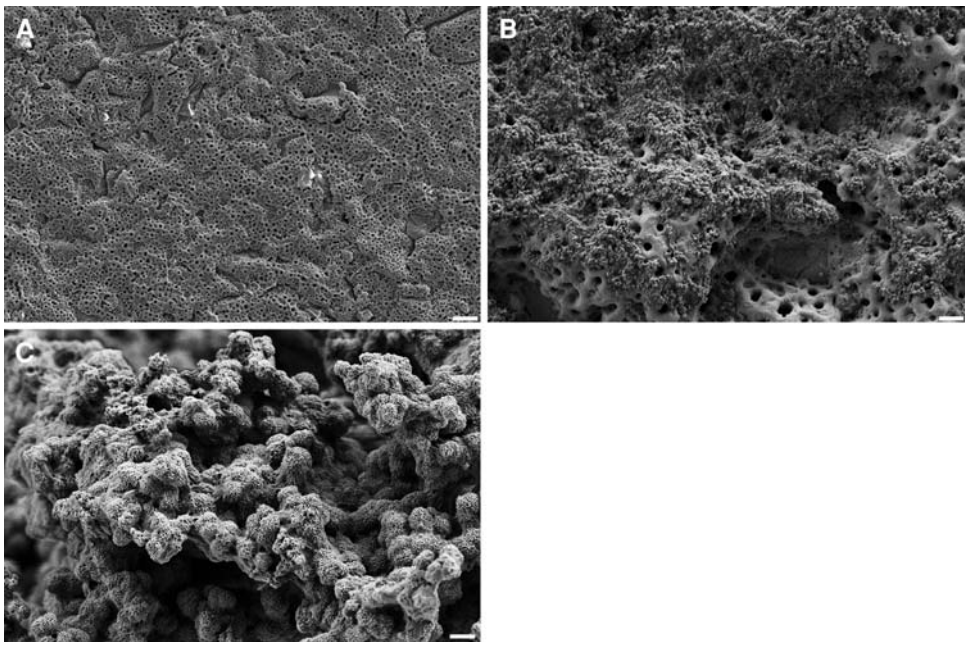

Fig. 3 SEM images of anodically oxidised specimens before (**a**, bar = 10 μm), and after SBF + fibrinogen immersion for 3 days (**a**, bar = 2 μm) and 4 weeks (bar = 2 μm)

3.2 SEM

The blasted controls and the hydroxyapatite coated controls showed a rather similar morphology as characterised with SEM (Figs. 1a, 5a). However, the surface structures of the alkali and heat treated, the anodically oxidised, and the fluoride modified specimens were more characteristic for each surface modification group (Figs. 2a, 3a, 4a).

A layer of apatite was detectable on all surface groups after 3 days of SBF + fibrinogen immersion (Figs. 1b, 2b, 3b, 4b, 5b). The layer seemed to be thin, but covered relatively large parts of the specimens. The degree of apatite coverage increased with immersion time (Fig. 4c). Furthermore, at 2–4 weeks of immersion, porous structures with sharp angled edges (Fig. 1c) as well as more globular structures (Figs. 2c, 3c, 5c) could be seen. It was hard to distinguish clear differences in apatite formation on the specimens with different surface preparations.

3.3 EDX

The titanium (Ti) coverage, as measured in terms of Ti atomic percentage (%) is presented in Fig. 6. In general, the titanium signals were highest for controls, and after

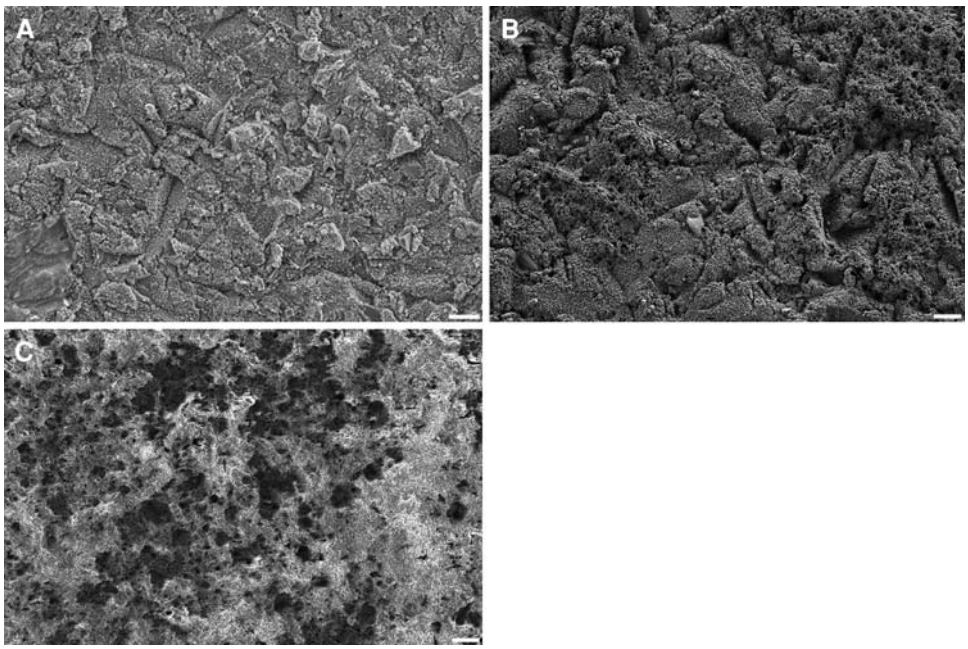

Fig. 4 SEM images of fluoride modified specimens before (**a**) and after SBF + fibrinogen immersion for 3 days (**b**) and 1 week (**c**). *Bars* correspond to 10 μm

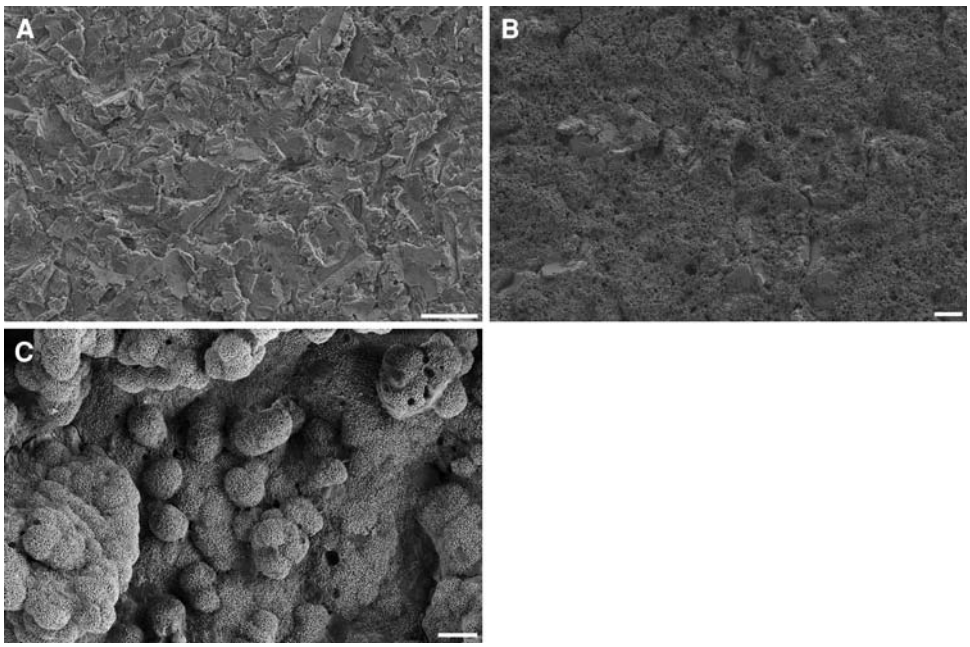

Fig. 5 SEM images of hydroxyapatite coated specimens before (**a**, bar = 20 μm), and after SBF + fibrinogen immersion for 3 days (**b**, bar = 10 μm) and 4 weeks (**c**, bar = 3 μm)

4 weeks of immersion no Ti could be detected on any surface type.

After 3 days of immersion the Ca/P mean ratios varied from 1.1 to 1.4, and increased to approximately 2.0 after 4 weeks' immersion, with the exception of the fluoride modified surface, which had a final Ca/P ratio of approximately 1.3 (Fig. 7).

The multivariate statistical analysis, comparing results from SBF immersion with or without fibrinogen, showed that the titanium signal was lower at 2 weeks immersion with fibrinogen added to the buffer ($P < 0.05$). Although not statistically significant, the titanium signal was lower also at 1 week immersion time for SBF + fibrinogen specimens (Fig. 8a).

Ca/P ratios at 2 and 4 weeks immersion times were not affected by the presence of fibrinogen ($P < 0.05$). However, when all surface groups were included in the multivariate analysis a statistically significant lower Ca/P ratio was shown for SBF + fibrinogen specimens at 1 week immersion time (Fig. 8b). When the analysis was repeated

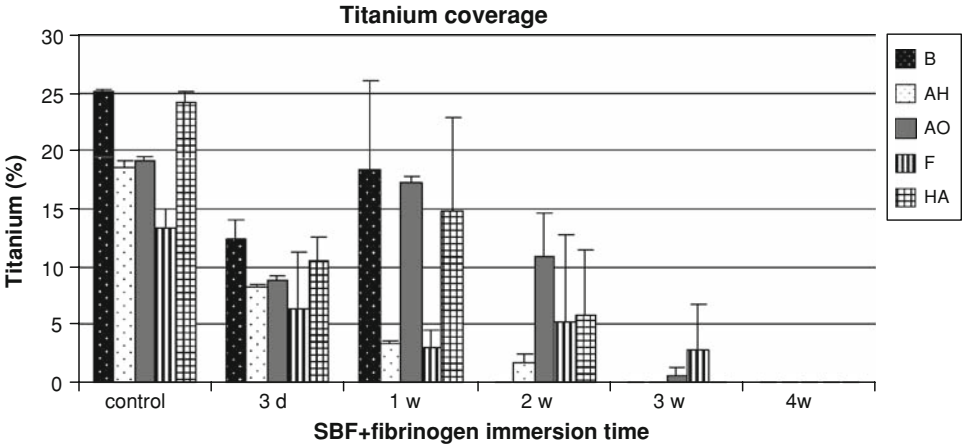

Fig. 6 Titanium coverage from EDX analyses. *B* blasted titanium, *AH* alkali and heat treated, *AO* anodically oxidised, *F* fluoridated, and *HA* hydroxyapatite coated. The bars are based on means calculated from two 3 mm^2 measurements from two different specimens

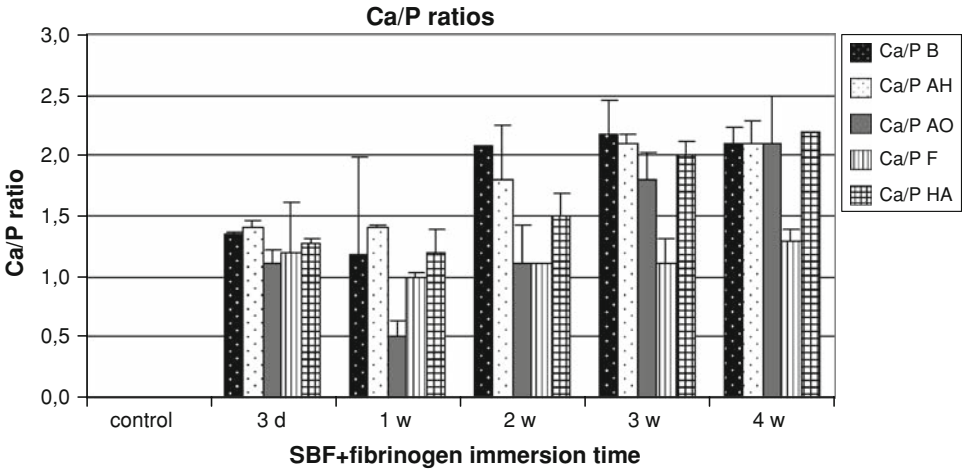

Fig. 7 Ca/P ratios from EDX analyses. *B* blasted titanium, *AH* alkali and heat treated, *AO* anodically oxidised, *F* fluoridated, and *HA* hydroxyapatite coated. The bars are based on means calculated from two 3 mm^2 measurements from two different specimens

without fluoride modified specimens, there was no longer any statistically significant difference between Ca/P ratios for SBF and SBF + fibrinogen specimens (Fig. 8c).

3.4 XPS

For blasted specimens, the N content reached its peak level at 3 days of SBF + fibrinogen immersion and thereafter decreased to lower concentrations (Fig. 9). The potentially bioactive surface modifications also showed a high N content after 3 days of SBF + fibrinogen immersion.

4 Discussion

All surfaces including the blasted controls showed early apatite formation after 3 days, and after 2 weeks the surfaces were more or less completely covered by calcium phosphates. When compared to earlier studies [23, 24], this result showed that fibrinogen stimulates calcium phosphates formation.

In the present study, all potentially bioactive surfaces were prepared by modifying a blasted control surface. As measured by the S_a mean values, the average height of structures seemed to be similar for the different surface groups (Table 1). However, surface roughness in terms of spatial (S_{ds}) and hybrid (S_{dr}) variation varied between groups. The largest mean values of the density of summits (S_{ds}) as well as the surface area enlargement (S_{dr}) were seen in the alkali and heat treated specimens, followed by the anodically oxidised specimens. Large S_{ds} and S_{dr} values theoretically might indicate a surface topography which promotes mineralisation via an increased number of nucleating sites. Negative skewness (S_{sk}) was found for all surface groups, which indicates surface topographies dominated by peaks rather than valleys. As all index parameters, the core fluid retention index (S_{ci}) lacks scalar information and shows a similar value independently on roughness level [33]. However, the index parameters can be used to qualitatively identify the shape of features. Since the range of S_{ci} values for optimal osseointegration possibly differ for different roughness scales, the use of a

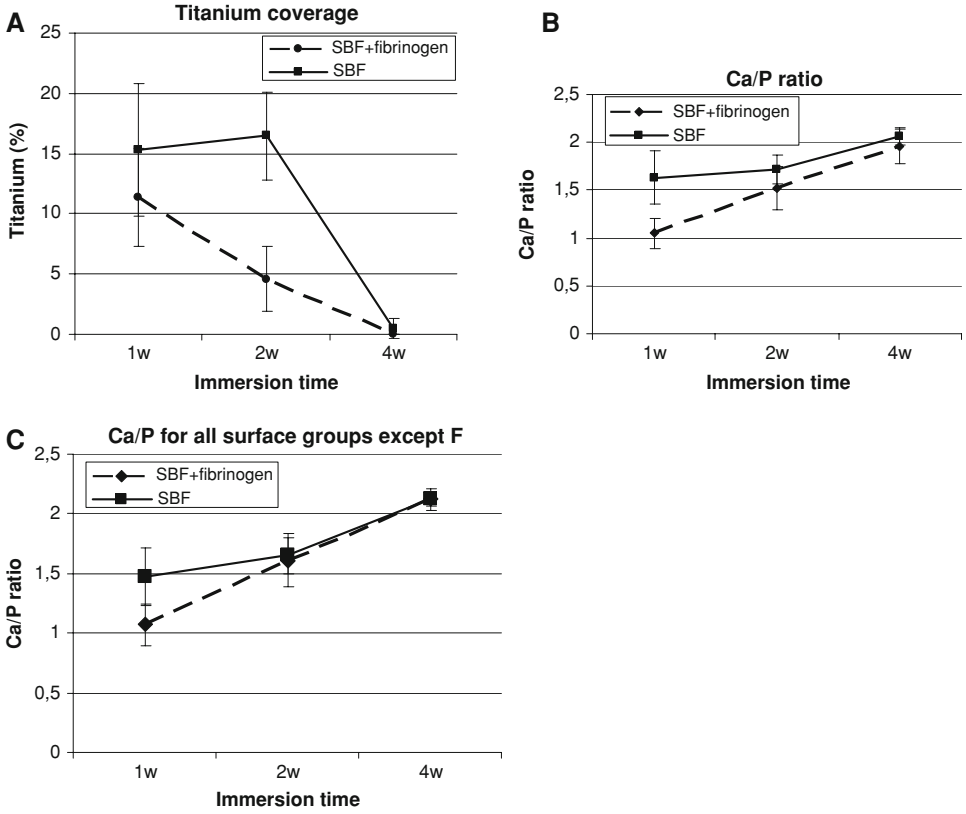

Fig. 8 Comparison of EDX results with results from an earlier study [23] using the same model but without fibrinogen added to the SBF buffer. Figures are mean values of all surface modification groups at a specific immersion time, with and without fibrinogen added to the solution. **a** Titanium coverage, **b** Ca/P ratios, and **c** Ca/P ratios for surface groups except fluoride modified specimens

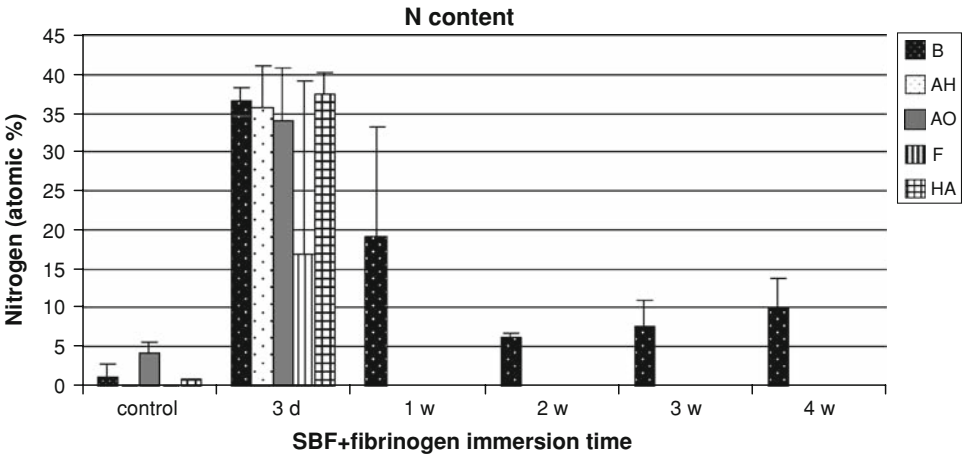

Fig. 9 Nitrogen content (atomic %) as measured with XPS. The bars are based on means calculated from two measurements from two different specimens

combination of different types of parameters facilitates the interpretation of surface roughness data. SEM images showing the varying surface morphology of the different potentially bioactive groups are provided in Figs. 1, 2, 3, 4 and 5.

The analytical depth of the EDX measurement with the current settings is approximately 0.5 μm. Since the coating on the hydroxyapatite specimens was noncontinuous and less than 100 nm thick, the controls did not show any Ca and P signals. However, with EDX the calcium phosphate formation could be indirectly studied via the titanium signals, and the Ca/P ratio could be calculated. The surface roughness of the specimens used in the present study corresponds to typical surface roughness of bone anchored implants, such as dental implants [5]. However, the amount of calcium phosphates formed on the specimens was not adequate for Thin film X-ray diffraction (TF-XRD) analysis of the relatively rough specimens, which otherwise would have given information on chemical structures of calcium phosphates formed. Previously, EDX has been used for calculation of the Ca/P ratio in order to estimate the relative prevalence of amorphous and crystalline calcium phosphates [27]. The stoichiometric Ca/P atomic ratios of octacalcium phosphate ($Ca_8H_2(PO_4)_6 \cdot 5H_2O$),

tricalcium phosphate ($Ca_3(PO_4)_2$), and hydroxyapatite ($Ca_5(PO_4)_3OH$) are 1.33, 1.5, and 1.67, respectively.

After 3 weeks of SBF immersion, a titanium signal was only detected for anodically oxidised and fluoride modified specimens, and after 4 weeks of immersion no titanium signal could be detected for any surface group. For blasted, anodically oxidised, and hydroxyapatite coated specimens, the titanium signal decreased with SBF immersion time, except that it was higher at 1 week than after 3 days (Fig. 6). Titanium signals were similar to or lower than titanium signals reported for the same surface groups immersed in SBF without proteins [23] (Fig. 8a). Titanium specimens immersed in SBF with albumin [24] showed higher titanium signals than specimens immersed in SBF with fibrinogen, indicating that fibrinogen promotes calcium phosphate formation more readily than does albumin. Nitrogen (N) could be detected with XPS, which is a more surface sensitive technique than EDX. However, EDX was selected for Ca and P analysis since it better reflects the average composition of the calcium phosphate layer. With the settings used for the analyses, the analytical depths of EDX and XPS are approximately 0.5 μm and 10 nm, respectively.

The N content of the amide group of the protein has earlier been used as an indirect method to show the presence of proteins [34]. In the present study, the nitrogen concentration reached its peak value after 3 days of immersion and thereafter decreased, which can be interpreted as meaning that fibrinogen adsorption is higher on titanium surfaces than on apatite.

Ca/P ratios varied between 1.0 and 1.5 after 3 days of SBF + fibrinogen immersion, and after 4 weeks immersion had reached approximately 2.0 for all surface groups except fluoride modified specimens, which had a Ca/P ratio of less than 1.5 (Fig. 7). These results are in accordance with Ca/P ratios reported for the same surface groups immersed in SBF without proteins [23], especially at immersion times of at least 2 weeks (Fig. 8c). Thus, it can be hypothesised that fibrinogen promotes mineralisation rather than influencing crystallinity.

Except for the fluoride modified surface, the amounts of apatite and the Ca/P ratios were quite similar for all the surfaces. The reason for this behaviour is probably the rapid coverage of fibrinogen on the surfaces. As can be seen from Fig. 9, the fibrinogen content on the surfaces after 3 days was very high. Thus, the effect of the different surface modifications on the crystallisation would have been diminished, since they were covered by fibrinogen.

SBFs are inorganic buffers, and provide simplified models for the in vivo situation. In vivo mineralisation takes place in a much more complex environment which includes proteins, cells, and other systemic factors. Blood plasma is about 91.5% water and 8.5% solutes. The solutes are mainly made up of proteins (7% of plasma by weight); the remaining plasma solutes include electrolytes (inorganic salts), nutrients (amino acids, glucose, fatty acids, and glycerol), regulatory substances (enzymes and hormones), gases (O_2, CO_2, and N_2), and wastes (e.g., urea, bilirubin) [25]. Plasma proteins include albumin (54%, size 70 kDa), globulins (38%), and fibrinogen (7%, size 340 kDa). Albumin is smaller than fibrinogen, a fact which could affect the proteins' interaction with mineralisation processes.

With respect to calcium and phosphate, body fluids are metastable; the concentration for these ions is well below that needed for spontaneous precipitation [26]. Thus, mineralisation requires either a mineralisation mechanism that locally elevates the concentration, or specific nucleating sites (e.g., proteins) that allow the formation from stable extracellular fluids of an initial nidus or seed [26].

The influence of proteins on mineralisation onto titanium surfaces has been studied previously. Lima et al. used Hanks buffer salt solution (HBSS) with albumin, and found that initially adsorbed albumin prevents the precipitation of a thick layer of tricalcium phosphate [35]. Another study, in which collagen was added to SBF, revealed that proteins may affect initial mineralisation times for anodically oxidised surfaces [36]. Furthermore, when fibronectin was added to HBSS, it was found that fibronectin strongly inhibited the formation of a calcium phosphate layer on titanium surfaces at a concentration of 0.05 mg/ml [37]. A study of tissue response to titanium implants in the rat tibia showed that the implant surface became covered in a layer rich in glycoconjugates, and that in contrast to bone matrix proteins such as osteocalcin and osteopontin, albumin showed no preferential accumulation at the bone–implant surface [38]. There are also other proteins, such as bone sialoprotein, whose role in initial mineralisation has been discussed [39, 40]. However, the clinical significance of the influence of proteins on mineralisation and apatite formation during bone formation is not yet fully understood, and should be studied using in vivo models.

Acknowledgements The authors gratefully acknowledge the financial support of the Hjalmar Svensson Research Foundation, the Swedish Medical Research Council, the Knut and Alice Wallenberg Foundation, the Wilhelm and Martina Lundgren Science Foundation, the Royal Society of Arts and Sciences in Göteborg, and the Ministry of Education & Human Resource Development, Republic of Korea and MediSci Tec Inc (biotechnology development project 2007-04306).

References

1. Wennerberg A. On surface roughness and implant incorporation. PhD thesis. Göteborg: Göteborg University; 1996.

2. Buser D. In: Brunette DM, Tengvall P, Textor M, Thomsen P, editors. Titanium in medicine. Berlin, Heidelberg: Springer; 2001. p. 875.
3. Predecki P, Auslender BA, Stephan JE, Mooney VL, Stanitski C. Attachment of bone to threaded implants by ingrowth and mechanical interlocking. J Biomed Mater Res. 1972;6:401–12. doi:10.1002/jbm.820060507.
4. Cooper L. A role for surface topography in creating and maintaining bone at titanium endosseous implants. J Prosthet Dent. 2000;84:522–34. doi:10.1067/mpr.2000.111966.
5. Albrektsson T, Wennerberg A. Oral implant surfaces: part 1—review focusing on topographic and chemical properties of different surfaces and in vivo responses to them. Int J Prosthodont. 2004;17:536–43.
6. Hansson S. Surface roughness parameters as predictors of anchorage strength in bone: a critical analysis. J Biomech. 2000;33:1297–303. doi:10.1016/S0021-9290(00)00045-2.
7. Webster TJ, Siegel RW, Bizios R. Osteoblast adhesion on nanophase ceramics. Biomaterials. 1999;20:1221–7. doi:10.1016/S0142-9612(99)00020-4.
8. Sato M, Aslani A, Sambito MA, Kalkhoran NM, Slamovich EB, Webster TJ. Nanocrystalline hydroxyapatite/titania coatings on titanium improves osteoblast adhesion. J Biomed Mater Res. 2008;84A:265–72. doi:10.1002/jbm.a.31469.
9. Hench LL. In: Yamamuro T, Hench LL, Wilson J, editors. Handbook of bioactive ceramics. Boca Raton: CRC Press; 1990. p. 7.
10. Kim HM, Miyaji F, Kokubo T, Nakamura T. Preparation of bioactive Ti and its alloys via simple chemical surface treatment. J Biomed Mater Res. 1996;32:409–17. doi:10.1002/(SICI)1097-4636(199611)32:3<409::AID-JBM14>3.0.CO;2-B.
11. Nishiguchi S, Nakamura T, Kobayashi M, Kim KM, Miyaji F, Kokubo T. The effect of heat treatment on bone-bonding ability of alkali treated titanium. Biomaterials. 1999;20:491–500. doi:10.1016/S0142-9612(98)90203-4.
12. Sul Y-T, Johansson CB, Byon E, Albrektsson T. The bone response of oxidized bioactive and non-bioactive titanium implants. Biomaterials. 2005;26:6720–30. doi:10.1016/j.biomaterials.2005.04.058.
13. Maitz MF, Poon RWY, Liu XY, Pham MT, Chu PK. Bioactivity of titanium following sodium plasma immersion ion implantation and deposition. Biomaterials. 2005;26:5465–73. doi:10.1016/j.biomaterials.2005.02.006.
14. Mello A, Hong Z, Rossi AM, Luan L, Farina M, Querido W, et al. Osteoblast proliferation on hydroxyapatite thin coatings produced by right angle magnetron sputtering. Biomed Mater. 2007;2:67–77. doi:10.1088/1748-6041/2/2/003.
15. Meirelles L, Arvidsson A, Andersson M, Kjellin P, Albrektsson T, Wennerberg A. Nano hydroxyapatite structures influence early bone formation. J Biomed Mater Res A. 2008;87:299–307. doi:10.1002/jbm.a.31744.
16. Ellingsen JE. Pre-treatment of titanium. Implants with fluoride improves their retention in bone. J Mater Sci: Mater Med. 1995;6:749–53. doi:10.1007/BF00134312.
17. Ellingsen JE, Johansson CB, Wennerberg A, Holmén A. Improved retention and bone to implant contact with fluoride-modified titanium implants. Int J Oral Maxillofac Implants. 2004;19:659–66.
18. Cooper L, Zhou Y, Takebe J, Guo J, Abron A, Holmén A, et al. Fluoride modification effects on osteoblast behaviour and bone formation at TiO_2 grit-blasted c.p. titanium endosseous implants. Biomaterials. 2006;27:926–36. doi:10.1016/j.biomaterials.2005.07.009.
19. Kokubo T, Kushitani H, Sakka S, Kitsugi T, Yamamuro T. Solutions able to reproduce in vivo surface–structure changes in bioactive glass–ceramic A-W3. J Biomed Mater Res. 1990;24:721–34. doi:10.1002/jbm.820240607.
20. Oyane A, Kim HK, Furuya T, Kokubo T, Miyazaki T, Nakamura T. Preparation and assessment of revised simulated body fluids. J Biomed Mater Res. 2003;65A:188–95. doi:10.1002/jbm.a.10482.
21. Berglundh T, Abrahamsson I, Lang NP, Lindhe J. De novo alveolar bone formation adjacent to endosseous implants: a model study in the dog. Clin Oral Implants Res. 2003;14:251–62. doi:10.1034/j.1600-0501.2003.00972.x.
22. Kokubo T, Takadama H. How useful is SBF in predicting in vivo bone bioactivity? Biomaterials. 2006;27:2907–15. doi:10.1016/j.biomaterials.2006.01.017.
23. Arvidsson A, Franke-Stenport V, Andersson M, Kjellin P, Sul Y-T, Wennerberg A. Formation of calcium phosphates on titanium implants with four different bioactive surface preparations. An in vitro study. J Mater Sci: Mater Med. 2007;18:1945–54. doi:10.1007/s10856-007-3097-3.
24. Stenport V, Kjellin P, Andersson M, Currie F, Sul Y-T, Wennerberg A, et al. Precipitation of calcium phosphate in the presence of albumin on titanium implants with four different possibly bioactive surface preparations. An in vitro study. J Mater Sci: Mater Med. 2008;19:3497–505. doi:10.1007/s10856-008-3517-z.
25. Tortora GJ, Grabowski SR. Principles of anatomy and physiology. 8th ed. New York: Harper Collins College Publishers; 1996. p. 552–77.
26. Davis WL. In: Davis WL, editor. Oral histology: cell structure and function. Philadelphia: WB Saunders Company; 1986. p. 73.
27. Takadama H, Kim HM, Kokubo T, Nakamura T. TEM-EDX study of mechanism of bone-like apatite formation on bioactive titanium metal in simulated body fluid. J Biomed Mater Res. 2001;57:441–8. doi:10.1002/1097-4636(20011205)57:3<441::AID-JBM1187>3.0.CO;2-B.
28. Kim HM, Miyaji F, Kokubo T, Nakamura T. Effect of heat treatment on apatite-forming ability of Ti metal induced by alkali treatment. J Mater Sci: Mater Med. 1997;8:341–7. doi:10.1023/A:1018524731409.
29. Kim HM, Miyaji F, Kokubo T, Nishiguchi S, Nakamura T. Graded surface structure of bioactive titanium prepared by chemical treatment. J Biomed Mater Res. 1999;45:100–7. doi:10.1002/(SICI)1097-4636(199905)45:2<100::AID-JBM4>3.0.CO;2-0.
30. Sul Y-T, Johansson CB, Jeong Y, Albrektsson T. The electrochemical oxide growth behaviour on titanium in acid and alkaline electrolytes. Med Eng Phys. 2001;23:329–46. doi:10.1016/S1350-4533(01)00050-9.
31. Sul Y-T, Johansson CB, Wennerberg A, Cho LR, Chang BS, Albrektsson T. Optimum surface properties of oxidized implants for reinforcement of osseointegration: surface chemistry, oxide thickness, porosity, roughness, and crystal structure. Int J Oral Maxillofac Implants. 2005;20:349–59.
32. Stout KJ, Sullivan PJ, Dong WP, Mainsah E, Luo N, Mathia T, Zahouani H. The development of methods for characterisation of roughness in three dimensions. EUR 15178 EN of commission of the European Communities (University of Birmingham, Birmingham, 1993).
33. Blunt L, Jiang X. Advanced techniques for assessment surface topography. London: Kogan Page Science; 2003. p. 17–41.
34. Zeng H, Chittur KK, Lacefield WR. Analysis of bovine serum albumin adsorption on calcium phosphate and titanium surfaces. Biomaterials. 1999;20:377–84. doi:10.1016/S0142-9612(98)00184-7.
35. Lima J, Sousa SR, Ferreira A, Barbosa MA. Interactions between calcium, phosphate, and albumin on the surface of titanium. J Biomed Mater Res. 2001;55:45–53. doi:10.1002/1097-4636(200104)55:1<45::AID-JBM70>3.0.CO;2-0.
36. Scharnweber D, Born R, Flade K, Roessler S, Stoelzel M, Worch H. Mineralization behaviour of collagen type I immobilized on different substrates. Biomaterials. 2004;25:2371–80. doi:10.1016/j.biomaterials.2003.09.025.

37. Serro AP, Fernandes AC, Saramago B. Calcium phosphate deposition on titanium surfaces in the presence of fibronectin. J Biomed Mater Res. 2000;49:345–52. doi:10.1002/(SICI)1097-4636(20000305)49:3<345::AID-JBM7>3.0.CO;2-R.
38. Nanci A, McCarthy GF, Zalzal S, Clokie CML, Warshawsky H, McKee MD. Tissue response to titanium implants in the rat tibia: ultrastructural, immunocytochemical and lectin-cytochemical characterization of the bone–titanium interface. Cells Mater. 1994;4:1–30.
39. Roach HI. Why does bone matrix contain non-collagenous proteins? The role of osteocalcin, osteonectin, osteopontin and bone sialoprotein in bone mineralisation and resorption. Cell Biol Int. 1994;18:617–26. doi:10.1006/cbir.1994.1088.
40. Ogata Y. Bone sialoprotein and its transcriptional regulatory mechanism. J Periodontal Res. 2008;43:127–35. doi:10.1111/j.1600-0765.2007.01014.x.